Local time-integration for Friedrich's systems
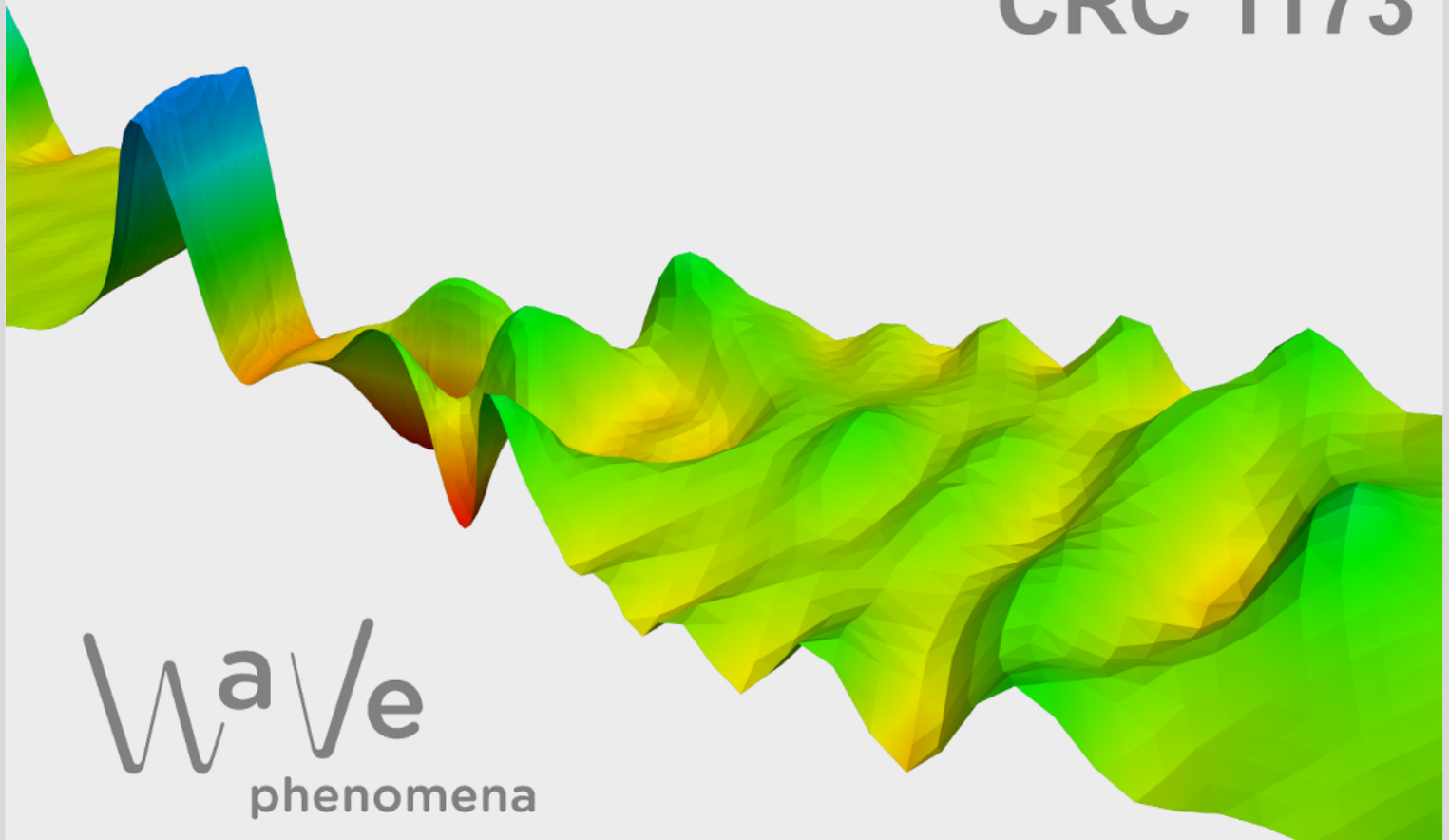
Marlis Hochbruck, Malik Scheifinger

KARLSRUHE INSTITUTE OF TECHNOLOGY

CRC 1173

Participating universities

UNIVERSITÄT BONN

Universität Stuttgart

EBERHARD KARLS
UNIVERSITÄT
TÜBINGEN

TU
WIEN

Funded by

DFG

LOCAL TIME-INTEGRATION FOR FRIEDRICHS' SYSTEMS[*]

MARLIS HOCHBRUCK[†] AND MALIK SCHEIFINGER[†]

Abstract. In this paper, we address the full discretization of Friedrichs' systems with a two-field structure, such as Maxwell's equations or the acoustic wave equation in div-grad form, cf. [14]. We focus on a discontinuous Galerkin space discretization applied to a locally refined mesh or a small region with high wave speed. This results in a stiff system of ordinary differential equations, where the stiffness is mainly caused by a small region of the spatial mesh. When using explicit time-integration schemes, the time step size is severely restricted by a few spatial elements, leading to a loss of efficiency. As a remedy, we propose and analyze a general leapfrog-based scheme which is motivated by [5]. The new, fully explicit, local time-integration method filters the stiff part of the system in such a way that its CFL condition is significantly weaker than that of the leapfrog scheme while its computational cost is only slightly larger. For this scheme, the filter function is a suitably scaled and shifted Chebyshev polynomial. While our main interest is in explicit local-time stepping schemes, the filter functions can be much more general, for instance, a certain rational function leads to the locally implicit method, proposed and analyzed in [24]. Our analysis provides sufficient conditions on the filter function to ensure full order of convergence in space and second order in time for the whole class of local time-integration schemes.

Key words. time integration, space discretization, Friedrichs' system, wave-type problems, local time-stepping methods, locally implicit methods, stability analysis, error analysis, discontinuous Galerkin

MSC codes. 65M12, 65M15, 65M22

1. Introduction. The aim of this paper is to construct and analyze a new local time-integration (LTI) method for the discontinuous Galerkin (dG) space discretization of Friedrichs' systems in a two-field structure. Using an explicit time-integrator like the leapfrog method on the full spatial domain necessitates satisfying a Courant–Friedrichs–Lewy (CFL) condition, meaning that the time stepsize τ is proportional to the inverse of the smallest diameter within the spatial mesh. On the other hand, implicit methods like the Crank-Nicolson method are unconditionally stable, but require the solution of large linear systems of equations. We are interested in problems, where the CFL condition is dominated by a small number of mesh elements, i.e., tiny elements or elements with a high wave speed. In this situation, standard explicit or implicit methods are inefficient. The basic idea of LTI methods is to use an explicit time-integrator, for example the leapfrog method, on the large, nonstiff part of the system and to couple it to a tailored method on the small, stiff part. The modified method can either be an explicit method with a weaker CFL condition (resulting in a local time-stepping (LTS) method) or an unconditionally stable implicit scheme (leading to a locally-implicit (LI) method). Overall one aims at using a method with a CFL condition which only depends on the nonstiff part of the system. Since the higher computational cost of the modified method arises only on a small part of the degrees of freedom, the construction leads to a problem adapted and efficient local time-integration scheme.

In recent years, many LTI schemes were introduced for different wave-type equations. LTS methods for the acoustic wave equation in second-order formulation were

---

[†]Institute for Applied and Numerical Mathematics, Karlsruhe Institute for Technology, 76131 Karlsruhe, Germany (marlis.hochbruck@kit.edu, malik.scheifinger@kit.edu).

constructed in [1, 6, 11, 12, 16, 17, 19, 20], for Maxwells equations in second-order formulation in [18, 26, 27, 29] and LI methods for Maxwells equations in [7, 8, 9, 13, 24, 25, 30, 32], for instance. Moreover, in [14] the LI method from [24] was generalized to Friedrichs' systems.

However, to the best of our knowledge fully explicit LTS methods for Friedrichs' systems have not been considered so far. Here, we construct and analyze a class of leapfrog-based LTI schemes motivated by [6]. We will show that the method is stable under a CFL condition which is independent of the stiff part of the problem and is of second-order in time and optimal order in space. As a special case, one variant of the LTI scheme corresponds to the LI method from [14] and the theoretical results reduce to the ones given there.

Outline. The paper is structured as follows. First, in Section 2, we briefly review Friedrichs' systems and introduce the notation which we will use throughout the paper.

Our main results are contained in Section 3. Here, we start with an introduction of the splitting of the discrete operators into a stiff and a nonstiff part. Then, we present the new LTI scheme based on the leapfrog method with a general filter function and study its stability. Important examples leading to LTS and LI methods are discussed in detail. For the whole class of methods, we prove stability if a time stepsize restriction based on properties of the filter function is satisfied. Moreover, we prove that LTI methods satisfy error bounds with optimal order in space and second-order in time.

At last, in Section 4, we present numerical experiments which substantiate our theoretical results for Maxwells equations. Moreover, we show that the LTS method outperforms the LI and the leapfrog method on these test problems.

2. Friedrichs' systems. Let $\Omega \subset \mathbb{R}^d$ be an open, polygonal domain and denote its boundary by $\Gamma = \partial\Omega$.

Following [14, §11.2] we consider the two-field structured Friedrichs' system

$$\text{(2.1a)} \qquad \partial_t u = \mathcal{L}_v v + g_u, \qquad\qquad \text{on } \Omega \times \mathbb{R}_+,$$
$$\text{(2.1b)} \qquad \partial_t v = \mathcal{L}_u u + g_v, \qquad\qquad \text{on } \Omega \times \mathbb{R}_+,$$
$$\qquad\qquad u(0) = u^0, \quad v(0) = v^0, \qquad\qquad \text{on } \Omega$$

with initial values u^0, v^0 and right-hand-side g. The Friedrichs' operators $\mathcal{L}_u$ and $\mathcal{L}_v$ are given as

$$\text{(2.2)} \qquad \mathcal{M}_v \mathcal{L}_u u = \sum_{i=1}^d L_i \partial_i u, \qquad \mathcal{M}_u \mathcal{L}_v v = \sum_{i=1}^d L_i^{\mathrm{T}} \partial_i v,$$

with $L_i \in \mathbb{R}^{m_v \times m_u}$ for $i = 0, \ldots, d$. The material tensors $\mathcal{M}_u \in L^\infty(\Omega)^{m_u \times m_u}$, $\mathcal{M}_v \in L^\infty(\Omega)^{m_v \times m_v}$ are assumed to be symmetric and positive definite, and $m_u, m_v \in \mathbb{N}$ denote the number of components of u and v. The boundary conditions of (2.1) are embodied into the domains $\mathcal{D}(\mathcal{L}_u)$ and $\mathcal{D}(\mathcal{L}_v)$, see [10, 14] for details. We further assume that the boundary conditions do not introduce damping, cf. [14, Assump. 11.8]. This leads to the important adjointness property

$$\text{(2.3)} \qquad \big(\mathcal{L}_u u, v\big) = -\big(u, \mathcal{L}_v v\big) \qquad \text{for all } u \in \mathcal{D}(\mathcal{L}_u), v \in \mathcal{D}(\mathcal{L}_v).$$

Special cases are linear Maxwells equations or the acoustic wave-equation in div-grad formulation, for details see [10, §7.1] or [14, §9.3].

2.1. Notation. Let $K \subseteq \mathbb{R}^d$ be open. For two vector-valued functions $u, \tilde{u} \in L^2(K)^{m_u}$ we denote the L^2-inner product by

$$\left(u, \tilde{u}\right)_{L^2(K)} = \int_K u \cdot \tilde{u} \, \mathrm{d}x$$

and the L^2-inner product weighted by $\mathcal{M}_u$ as

$$\left(u, \tilde{u}\right)_K = \left(u, \tilde{u}\right)_{\mathcal{M}_u, K} = \left(\mathcal{M}_u u, \tilde{u}\right)_{L^2(K)},$$

where we supress the indices $\mathcal{M}_u$ whenever possible. The inner product weighted by $\mathcal{M}_v$ is defined analogously. From the arguments of the inner product it is clear which weight is used. The induced norms are denoted accordingly.

Furthermore, we denote by ∂_i the ith weak derivative, $i = 1, \ldots, d$. Higher derivatives are denoted by $\partial^\alpha = \partial_1^{\alpha_1} \ldots \partial_d^{\alpha_d}$ for a multi index $\alpha \in \mathbb{N}_0^d$, and we write $|\alpha| = \alpha_1 + \cdots + \alpha_d$.

The Sobolev spaces in $L^2(K)$ are denoted as $H^\ell(K)$, $\ell \in \mathbb{N}_0$, and are equipped with the weighted norms

$$\|u\|_{\ell,K}^2 = \|u\|_{\mathcal{M}_u, \ell, K}^2 = \sum_{j=0}^\ell |u|_{\mathcal{M}_u, j, K}^2, \qquad |u|_{j,K}^2 = |u|_{\mathcal{M}_u, j, K}^2 = \sum_{|\alpha|=j} \|\partial^\alpha u\|_{\mathcal{M}_u, K}^2.$$

Again we suppress the index $\mathcal{M}_u$ whenever possible.

In what follows, we recall some notation and results from [10, 14]. We denote by $\mathcal{T}_h$ meshes of Ω which we assume to be admissible [10, Def. 1.57]. By h_K we denote the diameter of a cell $K \in \mathcal{T}_h$. We further define $h \in L^\infty(\Omega)$ by $h|_K = h_K$ and $h_{\max} = \max_K h_K$ as well as $h_{\min} = \min_K h_K$.

For each component of (2.1) we denote by

$$\mathbb{V}_h^u = \{u \in L^2(\Omega) \mid u|_K \in \mathbb{P}_d^k(K) \text{ for all } K \in \mathcal{T}_h\}^{m_u},$$
$$\mathbb{V}_h^v = \{v \in L^2(\Omega) \mid v|_K \in \mathbb{P}_d^k(K) \text{ for all } K \in \mathcal{T}_h\}^{m_v},$$

the spaces of broken polynomials of total degree at most k and the product space by $\mathbb{V}_h = \mathbb{V}_h^u \times \mathbb{V}_h^v$.

Furthermore, we symbolize the L^2-projection w.r.t. the weighted inner product $(\cdot, \cdot)_\Omega$ by $\pi_h \colon L^2(\Omega) \to \mathbb{V}_h$, see [14] for details.

At last, we recall the broken Sobolev spaces

$$H^\ell(\mathcal{T}_h) = \{u \in L^2(\Omega) \mid u|_K \in H^\ell(K) \text{ for all } K \in \mathcal{T}_h\}.$$

with weighted norms

$$\|u\|_{\ell,\mathcal{T}_h}^2 = \sum_{j=0}^\ell |u|_{j,\mathcal{T}_h}^2, \qquad |u|_{j,\mathcal{T}_h}^2 = \sum_{K \in \mathcal{T}_h} |u|_{j,K}^2.$$

3. Local time-integration. After a central-fluxes dG discretization [14, 15, 22], the spatially discrete wave-type problem (2.1) takes the form

(3.1a)	$\partial_t u_h = \mathcal{L}_{v,h} v_h + g_{u,h},$	on $\mathbb{R}_+$,
(3.1b)	$\partial_t v_h = \mathcal{L}_{u,h} u_h + g_{v,h},$	on $\mathbb{R}_+$,
(3.1c)	$u_h(0) = \pi_h u^0, \quad v_h(0) = \pi_h v^0, \quad g_h = \pi_h g,$	

where the discrete operators $\mathcal{L}_{u,h}, \mathcal{L}_{v,h}$ inherit the adjointness property (2.3), i.e.,

$$(3.2) \qquad \left(\mathcal{L}_{u,h} u_h, v_h\right)_\Omega = -\left(u_h, \mathcal{L}_{v,h} v_h\right)_\Omega \qquad \text{for all } u_h \in \mathbb{V}_h^u,\ v_h \in \mathbb{V}_h^v.$$

Before we present our local time-integration scheme, we follow [24] and split the mesh into two parts

$$(3.3) \qquad \mathcal{T}_h = \mathcal{T}_{h,f} \,\dot\cup\, \mathcal{T}_{h,c}.$$

The set $\mathcal{T}_{h,f}$ contains all elements with a small diameter or a high wave speed and the set $\mathcal{T}_{h,c}$ all others. We further define

$$(3.4) \qquad h_{c,\min} = \min_{K \in \mathcal{T}_{h,c}} h_K, \qquad h_{f,\min} = \min_{K \in \mathcal{T}_{h,f}} h_K.$$

Our approach necessitates an additional division of the mesh such that the set $\mathcal{T}_{h,m}$ contains also the neighbors of elements in $\mathcal{T}_{h,f}$ and $\mathcal{T}_{h,\mathrm{lf}}$ only contains coarse elements with coarse neighbors, i.e.,

$$\mathcal{T}_{h,m} = \{K \in \mathcal{T}_h \ :\ \exists K_f \in \mathcal{T}_{h,f} \text{ s.t. } K, K_f \text{ share a face}\},$$
$$\mathcal{T}_{h,\mathrm{lf}} = \mathcal{T}_h \setminus \mathcal{T}_{h,m}.$$

This one extra layer of coarse elements in $\mathcal{T}_{h,m}$ is essential to the independence of small mesh diameters or high wave speeds in the CFL condition as we will prove later on.

We further define the cutoff-operators

$$(3.5) \qquad \chi_m u = \begin{cases} u, & \text{on } K \in \mathcal{T}_{h,m}, \\ 0, & \text{on } K \in \mathcal{T}_{h,\mathrm{lf}}, \end{cases} \qquad \text{and} \qquad \chi_{\mathrm{lf}} u = \begin{cases} 0, & \text{on } K \in \mathcal{T}_{h,m}, \\ u, & \text{on } K \in \mathcal{T}_{h,\mathrm{lf}}. \end{cases}$$

Now we are able to propose our local time-integration method. With a smooth function $\Psi\colon [0,\infty) \to \mathbb{R}$ satisfying $\Psi(0) = 1$, the fully discrete local time-integration scheme is defined as

$$(3.6a) \qquad \bar{v}_h^{n+1/2} - v_h^n = \tfrac{\tau}{2}\mathcal{L}_{u,h} u_h^n + \tfrac{\tau}{2} g_{v,h}^{n+1/2},$$

$$(3.6b) \qquad u_h^{n+1} - u_h^n = \tau\mathbf{\Psi}\left(\mathcal{L}_{v,h}\bar{v}_h^{n+1/2} + g_{u,h}^{n+1/2}\right),$$

$$(3.6c) \qquad v_h^{n+1} - \bar{v}_h^{n+1/2} = \tfrac{\tau}{2}\mathcal{L}_{u,h} u_h^{n+1} + \tfrac{\tau}{2} g_{v,h}^{n+1/2},$$

$$(3.6d) \qquad \mathbf{\Psi} = \Psi(-\tau^2 \mathcal{L}_{v,h}\chi_m \mathcal{L}_{u,h})\,.$$

Note that in [6] we used the notation $\widehat{\Psi}$ instead of Ψ.

We denote by

$$(3.7) \qquad g_h^{n+1/2} = \tfrac{1}{2}(g_h^{n+1} + g_h^n)$$

the average of g_h at two consecutive time steps. Note that the filter function $\mathbf{\Psi}$ and hence the modified method only work on $\mathcal{T}_{h,m}$ plus coupling and that for $\Psi \equiv 1$, the scheme reduces to the leapfrog scheme.

The remaining part of this paper is devoted to the proof of the following full-discretization error estimate.

THEOREM 3.1. *For* $x_h^n = \begin{pmatrix} u_h^n & v_h^n \end{pmatrix}$ *given by* (3.6) *with* τ *satisfying a CFL condition independent of* $h_{f,\min}$ *and a sufficiently regular solution* $x = \begin{pmatrix} u & v \end{pmatrix}$ *of* (2.1) *we obtain*

$$\|x(t^n) - x_h^n\|_\Omega \leq C(\tau^2 + h_{\max}^k) \tag{3.8}$$

with a constant C *independent of* τ *and* $h_{\max}$.

Details on the CFL condition will be given later.

3.1. Stability. In the following, we assume that $\boldsymbol{\Psi}$ defined in (3.6d) is invertible, which is indeed the case under a certain restriction on the time stepsize as we will later see. We start by rewriting (3.6) into a system inspired by the analysis of the Crank-Nicolson method [24] imitating a discrete semi-group technique. To do so, we define

$$\boldsymbol{\mathcal{R}}_\pm = \begin{pmatrix} \boldsymbol{\Theta} & \pm\frac{\tau}{2}\mathcal{L}_{v,h} \\ \pm\frac{\tau}{2}\mathcal{L}_{u,h} & \mathcal{I}_v \end{pmatrix} - \frac{\tau^2}{4}\begin{pmatrix} -\mathcal{L}_{v,h}\chi_{\mathrm{lf}}\mathcal{L}_{u,h} & 0 \\ 0 & 0 \end{pmatrix} \tag{3.9a}$$

with

$$\boldsymbol{\Theta} = \Theta(-\tau^2 \mathcal{L}_{v,h}\chi_m\mathcal{L}_{u,h}), \tag{3.9b}$$

$$\Theta(z) = \Psi(z)^{-1}\big(1 - \tfrac{z}{4}\Psi(z)\big) = \frac{1}{\Psi(z)} - \frac{z}{4}, \qquad \Theta(0) = 1. \tag{3.9c}$$

In Table 1, we collect special choices of Ψ and Θ together with certain parameters, which we will introduce later for the analysis. More details will be given in Section 3.3 below.

LEMMA 3.2. *The approximations* $x_h^n = \begin{pmatrix} u_h^n & v_h^n \end{pmatrix}$ *of the local time-integration scheme* (3.6) *satisfy*

$$\boldsymbol{\mathcal{R}}_- x_h^{n+1} = \boldsymbol{\mathcal{R}}_+ x_h^n + \tau g_h^{n+1/2}, \qquad g_h^{n+1/2} = \begin{pmatrix} g_{u,h}^{n+1/2} \\ g_{v,h}^{n+1/2} \end{pmatrix}. \tag{3.10}$$

A key idea is to split $\boldsymbol{\mathcal{R}}_\pm$ into a positive definite operator $\boldsymbol{\Theta}_\mathcal{I}$, a skew-adjoint operator $\mathcal{L}_h$, and a self-adjoint, positive semidefinite perturbation operator $\boldsymbol{\mathcal{D}}_{\mathrm{lf}}$ via

$$\boldsymbol{\mathcal{R}}_\pm = \boldsymbol{\Theta}_\mathcal{I} \pm \tfrac{\tau}{2}\mathcal{L}_h - \tfrac{\tau^2}{4}\boldsymbol{\mathcal{D}}_{\mathrm{lf}}, \tag{3.11a}$$

where

$$\boldsymbol{\Theta}_\mathcal{I} = \begin{pmatrix} \boldsymbol{\Theta} & 0 \\ 0 & \mathcal{I}_v \end{pmatrix}, \quad \mathcal{L}_h = \begin{pmatrix} 0 & \mathcal{L}_{v,h} \\ \mathcal{L}_{u,h} & 0 \end{pmatrix}, \quad \boldsymbol{\mathcal{D}}_{\mathrm{lf}} = \begin{pmatrix} -\mathcal{L}_{v,h}\chi_{\mathrm{lf}}\mathcal{L}_{u,h} & 0 \\ 0 & 0 \end{pmatrix}. \tag{3.11b}$$

Here, the adjointness condition (3.2) directly implies that $\mathcal{L}_h$ is skew-adjoint, $\boldsymbol{\mathcal{D}}_{\mathrm{lf}}$ and $\boldsymbol{\Theta}$ are self-adjoint, and that $\boldsymbol{\mathcal{D}}_{\mathrm{lf}}$ is positive semidefinite. However, the definiteness of $\boldsymbol{\Theta}_\mathcal{I}$ is only guaranteed for special choices of Θ (see Table 1) or under additional conditions on its argument $-\tau^2\mathcal{L}_{v,h}\chi_m\mathcal{L}_{u,h}$ in (3.9b). To ensure this, we introduce additional notation.

DEFINITION 3.3. *Let* $\Psi\colon [0,\infty) \to \mathbb{R}$ *be a smooth function satisfying* $\Psi(0) = 1$ *and consider* Θ *defined in* (3.9c). *For a constant* $c_\Theta \in (0,1]$ *we define* $\beta_\Psi = \beta_\Psi(c_\Theta) \in (0,\infty]$ *as the maximum value such that*

$$0 < \Psi(z) \leq 1 \quad \text{and} \quad \Theta(z) \geq c_\Theta \qquad \text{for all } z \in [0, \beta_\Psi^2] \cap \mathbb{R}, \tag{3.12}$$

and $\beta_\Psi = \infty$, *if* (3.12) *holds for all* $z \geq 0$.

	Ψ	Θ	φ	β_Ψ^2	c_Θ	C_φ
Leapfrog	1	$1 - \frac{z}{4}$	$-\frac{1}{4}$	$4(1 - c_\Theta)$	$1 - \vartheta^2$	$\frac{1}{4}$
Crank-Nicolson	$(1 + \frac{z}{4})^{-1}$	1	0	∞	1	0
Leapfrog-Chebychev	(3.41)	(3.9c)	(3.32a)	(3.42b)	(3.42a)	(3.42b)

Table 1: Examples for filter functions with corresponding constants.

The parameters β_Ψ^2 and c_Θ directly enter the CFL conditions to ensure stability of the scheme.

DEFINITION 3.4. *For given $\vartheta, \vartheta_c \in (0, 1]$ we define*

$$(3.13a) \qquad \tau_{\mathrm{CFL},\Psi}^2 = \frac{\beta_\Psi^2}{\|\mathcal{L}_{v,h}\chi_m\mathcal{L}_{u,h}\|},$$

$$(3.13b) \qquad \tau_{\mathrm{CFL,lf,c}}^2 = \tau_{\mathrm{CFL,lf,c}}^2(\vartheta_c) = \frac{4c_\Theta\vartheta_c^2}{\|\mathcal{L}_{v,h}\chi_{\mathrm{lf}}\mathcal{L}_{u,h}\|},$$

and

$$(3.14) \qquad \tau_{\mathrm{CFL,lf}}^2 = \tau_{\mathrm{CFL,lf}}^2(\vartheta) = \frac{4\vartheta^2}{\|\mathcal{L}_{v,h}\mathcal{L}_{u,h}\|}.$$

Recall that the leapfrog scheme on the whole spatial domain is stable if $\tau \le \tau_{\mathrm{CFL,lf}}$. Obviously, we aim at choosing Ψ in such a way that the CFL condition of the local time-integration method is significantly relaxed compared to the leapfrog scheme. For the dependence of the CFL condition on the submeshes and the material parameters, note that

$$\|\mathcal{L}_{v,h}\chi_{\mathrm{lf}}\mathcal{L}_{u,h}\| \lesssim h_{c,\min}^{-2}, \qquad \|\mathcal{L}_{v,h}\chi_m\mathcal{L}_{u,h}\| \lesssim h_{f,\min}^{-2},$$

with constants that depend on the largest eigenvalue of $\mathcal{M}_u^{-1}L_i^{\mathrm{T}}\mathcal{M}_v^{-1}L_i$, $i = 1, \dots, d$, on $\mathcal{T}_{h,c}$ and $\mathcal{T}_{h,f}$ respectively, cf. [23, Eq. 6] or [10, Lem. 7.32]. Roughly speaking, the largest eigenvalues scale like the inverse of the product of the smallest eigenvalues of $\mathcal{M}_u$ and $\mathcal{M}_v$ on the respective submeshes. It is important to note that the eigenvalues of $\mathcal{L}_{v,h}\chi_{\mathrm{lf}}\mathcal{L}_{u,h}$ and hence $\tau_{\mathrm{CFL,lf,c}}$ are independent of the material parameters and the diameters within the fine mesh $\mathcal{T}_{h,f}$, cf. [14, 24] for details.

LEMMA 3.5. *For $\tau \le \tau_{\mathrm{CFL},\Psi}$ defined (3.13a), the operator Θ induces a norm $\|\cdot\|_\Theta$ such that for all $u_h \in \mathbb{V}_h^u$ we have*

$$(3.15) \qquad c_\Theta\|u_h\|_\Omega^2 \le \|u_h\|_\Theta^2 = \left(\Theta u_h, u_h\right)_\Omega.$$

Proof. The statement follows immediately from (3.12) since we can bound the eigenvalues z of $-\tau^2\mathcal{L}_{v,h}\chi_m\mathcal{L}_{u,h}$ by β_Ψ^2 if $\tau \le \tau_{\mathrm{CFL},\Psi}$. $\square$

Lemma 3.5 implies that $\Theta_\mathcal{I}$ defined in (3.9b) is also self-adjoint and positive definite for $\tau \le \tau_{\mathrm{CFL},\Psi}$ and hence it induces a norm $\|\cdot\|_{\Theta_\mathcal{I}}$ on $\mathbb{V}_h$.

Using both CFL conditions in (3.13) we can bound the action of the operators $\mathcal{R}_\pm$ defined in (3.9a) from below.

LEMMA 3.6. *Let $\vartheta_c \in (0,1)$ and $\tau \leq \min\{\tau_{\mathrm{CFL,lf,c}}(\vartheta_c), \tau_{\mathrm{CFL},\Psi}\}$ satisfy the CFL conditions* (3.13). *Then we have*

$$(3.16) \qquad c_\Theta(1 - \vartheta_c^2)\|u_h\|_\Omega^2 + \|v_h\|_\Omega^2 \leq \left(\mathcal{R}_\pm x_h, x_h\right)_\Omega.$$

for all $x_h = \begin{pmatrix} u_h & v_h \end{pmatrix} \in \mathbb{V}_h$.

Proof. Let $x_h = \begin{pmatrix} u_h & v_h \end{pmatrix} \in \mathbb{V}_h$. Using (3.11b) and (3.13b) we obtain

$$\tfrac{\tau^2}{4}\left(\mathcal{D}_{\mathrm{lf}} x_h, x_h\right)_\Omega = -\tfrac{\tau^2}{4}\left(\mathcal{L}_{v,h}\chi_{\mathrm{lf}}\mathcal{L}_{u,h}u_h, u_h\right)_\Omega \leq c_\Theta \vartheta_c^2 \|u_h\|_\Omega^2,$$

and thus with (3.11a) and (3.15)

$$\begin{aligned} \left(\mathcal{R}_\pm x_h, x_h\right)_\Omega &= \left(\Theta u_h, u_h\right)_\Omega + \|v_h\|_\Omega^2 - \tfrac{\tau^2}{4}\left(\mathcal{D}_{\mathrm{lf}} x_h, x_h\right)_\Omega \\ &\geq c_\Theta(1 - \vartheta_c^2)\|u_h\|_\Omega^2 + \|v_h\|_\Omega^2. \end{aligned}$$

This proves the statement. $\qquad\square$

In the next Lemma 3.7 we show that the CFL condition for the local time-integration scheme (3.6) can not become stronger than that of the leapfrog scheme used on the whole grid.

LEMMA 3.7. *Let $\vartheta \in (0,1)$, $x_h = \begin{pmatrix} u_h & v_h \end{pmatrix} \in \mathbb{V}_h$, and $\tau \leq \tau_{\mathrm{CFL,lf}}(\vartheta)$ defined in* (3.14). *Moreover, assume that $0 < \Psi(z) \leq 1$ holds for all $z \in [0, 4]$. Then we have*

$$(3.17) \qquad \left(\mathcal{R}_\pm x_h, x_h\right)_\Omega \geq (1 - \vartheta^2)\|u_h\|_\Omega^2 + \|v_h\|_\Omega^2.$$

Proof. By assumption, Ψ is invertible since the leapfrog CFL condition (3.14) implies $\| - \tau^2 \mathcal{L}_{v,h}\mathcal{L}_{u,h}\|_\Omega \leq 4\vartheta^2 \leq 4$ and thus $\left(\Psi^{-1}u_h, u_h\right)_\Omega \geq \|u_h\|_\Omega^2$. Using (3.9c) we can write

$$\begin{aligned} \Theta + \tfrac{\tau^2}{4}\mathcal{L}_{v,h}\chi_{\mathrm{lf}}\mathcal{L}_{u,h} &= \Psi^{-1} + \tfrac{\tau^2}{4}\left(\mathcal{L}_{v,h}\chi_m\mathcal{L}_{u,h} + \mathcal{L}_{v,h}\chi_{\mathrm{lf}}\mathcal{L}_{u,h}\right) \\ &= \Psi^{-1} + \tfrac{\tau^2}{4}\mathcal{L}_{v,h}\mathcal{L}_{u,h}. \end{aligned}$$

From (3.9a) and the CFL condition (3.14) we conclude

$$\begin{aligned} \left(\mathcal{R}_\pm x_h, x_h\right)_\Omega &= \left((\Theta + \tfrac{\tau^2}{4}\mathcal{L}_{v,h}\chi_{\mathrm{lf}}\mathcal{L}_{u,h})u_h, u_h\right)_\Omega + \|v_h\|_\Omega^2 \\ &\geq (1 - \vartheta^2)\|u_h\|_\Omega^2 + \|v_h\|_\Omega^2. \end{aligned}$$

This completes the proof. $\qquad\square$

Lemma 3.6 and the splitting of $\mathcal{R}_\pm$ in (3.9a) lead to the following properties.

LEMMA 3.8. *Let $\tau \leq \min\{\tau_{\mathrm{CFL},\Psi}, \tau_{\mathrm{CFL,lf,c}}\}$ defined in* (3.13) *for some $\vartheta_c \in (0,1)$. Then, for $x_h, y_h \in \mathbb{V}_h$ and $\mathcal{R} = \mathcal{R}_-^{-1}\mathcal{R}_+$ we have for $n = 0, 1, 2, \ldots$ the identities*

$$(3.18\mathrm{a}) \qquad\qquad \left(\mathcal{R}_- x_h, y_h\right)_\Omega = \left(x_h, \mathcal{R}_+ y_h\right)_\Omega,$$

$$(3.18\mathrm{b}) \qquad\qquad \left(\mathcal{R}_- \mathcal{R}^n x_h, \mathcal{R}^n x_h\right)_\Omega = \left(\mathcal{R}_- x_h, x_h\right)_\Omega,$$

$$(3.18\mathrm{c}) \qquad \left(\mathcal{R}_- \mathcal{R}^n \mathcal{R}_-^{-1} x_h, \mathcal{R}^n \mathcal{R}_-^{-1} x_h\right)_\Omega = \left(\mathcal{R}_-^{-1} x_h, x_h\right)_\Omega,$$

and in addition the bounds

$$(3.19\mathrm{a}) \qquad\qquad \|\mathcal{R}^n x_h\|_\Omega \leq C_{stb,c}\|x_h\|_{\Theta_{\mathcal{I}}},$$

$$(3.19\mathrm{b}) \qquad\qquad \|\mathcal{R}^n \mathcal{R}_-^{-1} x_h\|_\Omega \leq C_{stb,c}\|x_h\|_\Omega,$$

$$(3.19\mathrm{c}) \qquad\qquad \|\mathcal{R}_\pm^{-1} x_h\|_\Omega \leq \|x_h\|_\Omega,$$

with $C_{stb,c} = (c_\Theta(1 - \vartheta_c^2))^{-1/2}$.

Proof. The adjointness property (3.18a) follows from the skew-adjointness of $\mathcal{L}_h$ and the self-adjointness of $\mathcal{L}_{v,h}\chi_{\mathrm{lf}}\mathcal{L}_{u,h}$, while (3.18b) can be seen by induction with

$$
\begin{aligned}
\left(\mathcal{R}_-\mathcal{R}x_h, \mathcal{R}x_h\right)_\Omega &= \left(\mathcal{R}_+x_h, \mathcal{R}x_h\right)_\Omega \\
&= \left(x_h, \mathcal{R}_-\mathcal{R}x_h\right)_\Omega \\
&= \left(x_h, \mathcal{R}_+x_h\right)_\Omega \\
&= \left(\mathcal{R}_-x_h, x_h\right)_\Omega.
\end{aligned}
$$

One can easily verify that the inverses are given by

$$
\begin{aligned}
\mathcal{R}_\pm^{-1} &= \begin{pmatrix} \boldsymbol{\Psi} & \mp\frac{\tau}{2}\boldsymbol{\Psi}\mathcal{L}_{v,h} \\ \mp\frac{\tau}{2}\mathcal{L}_{u,h}\boldsymbol{\Psi} & \mathcal{I}_v + \frac{\tau^2}{4}\mathcal{L}_{u,h}\boldsymbol{\Psi}\mathcal{L}_{v,h} \end{pmatrix} \\
(3.20) \qquad &= \begin{pmatrix} \boldsymbol{\Psi} & \\ & \mathcal{I}_v + \frac{\tau^2}{4}\mathcal{L}_{u,h}\boldsymbol{\Psi}\mathcal{L}_{v,h} \end{pmatrix} \mp \frac{\tau}{2}\begin{pmatrix} & \boldsymbol{\Psi}\mathcal{L}_{v,h} \\ \mathcal{L}_{u,h}\boldsymbol{\Psi} & \end{pmatrix}.
\end{aligned}
$$

These are decompositions of $\mathcal{R}_\pm^{-1}$ into their symmetric and skew-symmetric parts.

Replacing x_h by $\mathcal{R}_-^{-1}x_h$ in (3.18b) proves (3.18c). Furthermore, (3.16) and (3.18b) imply

$$
\begin{aligned}
c_\Theta(1-\vartheta_c^2)\|\mathcal{R}^n x_h\|_\Omega^2 &\leq \left(\mathcal{R}_-\mathcal{R}^n x_h, \mathcal{R}^n x_h\right)_\Omega \\
&= \left(\mathcal{R}_-x_h, x_h\right)_\Omega \\
&= \|x_h\|_{\boldsymbol{\Theta}_\mathcal{I}}^2 - \left(\mathcal{D}_{\mathrm{lf}}x_h, x_h\right)_\Omega \leq \|x_h\|_{\boldsymbol{\Theta}_\mathcal{I}}^2,
\end{aligned}
$$

where we have used the positive semi-definiteness of $\mathcal{D}_{\mathrm{lf}}$ in the last estimate. This proves (3.19a).

By (3.12), $\boldsymbol{\Psi}$ is positive definite if the CFL condition (3.13a) is satisfied. Thus we have with the adjointness property (3.2)

$$
\left(\mathcal{L}_{u,h}\boldsymbol{\Psi}\mathcal{L}_{v,h}v_h, v_h\right)_\Omega = -\left(\boldsymbol{\Psi}\mathcal{L}_{v,h}v_h, \mathcal{L}_{v,h}v_h\right)_\Omega \leq 0
$$

which shows

$$
\begin{aligned}
\left(\mathcal{R}_\pm^{-1}x_h, x_h\right)_\Omega &= \left(\boldsymbol{\Psi}u_h, u_h\right)_\Omega + \left(v_h, v_h\right)_\Omega + \frac{\tau^2}{4}\left(\mathcal{L}_{u,h}\boldsymbol{\Psi}\mathcal{L}_{v,h}v_h, v_h\right)_\Omega \\
&\leq \|x_h\|_\Omega^2.
\end{aligned}
$$

and with this (3.19c). Using (3.16), (3.18c) and (3.19c) shows

$$
\begin{aligned}
c_\Theta(1-\vartheta_c^2)\|\mathcal{R}^n\mathcal{R}_-^{-1}x_h\|_\Omega^2 &\leq \left(\mathcal{R}_-\mathcal{R}^n\mathcal{R}_-^{-1}x_h, \mathcal{R}^n\mathcal{R}_-^{-1}x_h\right)_\Omega \\
&= \left(\mathcal{R}_-^{-1}x_h, x_h\right)_\Omega \\
&\leq \|x_h\|_\Omega^2
\end{aligned}
$$

and hence (3.19b). $\qquad\square$

With the previous Lemma 3.8 we conclude the following stability estimate.

LEMMA 3.9 (Stability). *Let x_h^{n+1} be defined in (3.10). Under the same assumptions as in Lemma 3.8 the numerical solution is bounded by*

$$
(3.21) \qquad \|x_h^{n+1}\|_\Omega \leq C_{stb,c}\left(\|x_h^0\|_{\boldsymbol{\Theta}_\mathcal{I}} + \tau\sum_{j=0}^n \|g_h^{j+1/2}\|_\Omega\right).
$$

Proof. Since $\boldsymbol{\mathcal{R}}_-^{-1}$ is invertible, the scheme (3.10) is equivalent to

$$x_h^{n+1} = \boldsymbol{\mathcal{R}} x_h^n + \tau \boldsymbol{\mathcal{R}}_-^{-1} g_h^{n+1/2}, \qquad \boldsymbol{\mathcal{R}} = \boldsymbol{\mathcal{R}}_-^{-1} \boldsymbol{\mathcal{R}}_+.$$

Then, the discrete variation-of-constants formula yields

$$(3.22) \qquad x_h^{n+1} = \boldsymbol{\mathcal{R}}^{n+1} x_h^0 + \tau \sum_{j=0}^{n} \boldsymbol{\mathcal{R}}^{n-j} \boldsymbol{\mathcal{R}}_-^{-1} g_h^{j+1/2}.$$

The claim now follows from (3.19a) and (3.19b) and the triangle inequality. $\square$

3.2. Error analysis of the local time-integration scheme. In the following we denote the exact solution of (2.1) evaluated at time t^n by

$$(3.23) \qquad \widehat{x}^n = x(t^n), \qquad x = \begin{pmatrix} u & v \end{pmatrix}.$$

The error of the full discretization is given by

$$(3.24) \qquad e^n = \widehat{x}^n - x_h^n = e_\pi^n + e_h^n, \qquad e_\pi^n = \widehat{x}^n - \pi_h \widehat{x}^n, \qquad e_h^n = \pi_h \widehat{x}^n - x_h^n,$$

where e_π^n denotes the L^2-projection error and e_h^n the discretization error respectively.

To define defects δ_h^{n+1} we insert the L^2-projected exact solution into the numerical scheme (3.10). This yields

$$(3.25) \qquad \boldsymbol{\mathcal{R}}_- \pi_h \widehat{x}^{n+1} = \boldsymbol{\mathcal{R}}_+ \pi_h \widehat{x}^n + \tau g_h^{n+1/2} + \tau \delta_h^{n+1}.$$

Subtracting (3.10) from (3.25) yields the error recursion

$$(3.26) \qquad \boldsymbol{\mathcal{R}}_- e_h^{n+1} = \boldsymbol{\mathcal{R}}_+ e_h^n + \tau \delta_h^{n+1}.$$

This recursion is of the same form as (3.10). Hence, we can apply Lemma 3.9 to bound the error. Unfortunately, it will turn out later, that we need a more careful inspection of the defects to deal with the cutoff functions within the Friedrichs' operators. Otherwise, this would lead to suboptimal error bounds.

THEOREM 3.10. *Let* $\tau \leq \min\{\tau_{\mathrm{CFL},\Psi}, \tau_{\mathrm{CFL,lf},c}\}$ *defined in (3.13) for some* $\vartheta_c \in (0, 1)$. *If one can decompose the defect into*

$$(3.27a) \qquad \delta_h^j = \delta_{h,s}^j + \mathcal{L}_h \delta_{h,\mathcal{L}_h}^j \quad \text{with} \quad \delta_{h,\mathcal{L}_h}^j = \begin{pmatrix} 0 \\ \delta_{h,v,\mathcal{L}_h}^j \end{pmatrix},$$

then it holds

$$\|e_h^{n+1}\|_\Omega \leq C_{stb,\,c} \left(\|e_h^0\|_{\Theta_\mathcal{I}} + \tau \sum_{j=1}^{n+1} \|\delta_{h,s}^j\|_\Omega + \|\delta_{h,v,\mathcal{L}_h}^1\|_\Omega + \tau \sum_{j=2}^{n+1} \|\partial_\tau \delta_{h,v,\mathcal{L}_h}^j\|_\Omega \right)$$

$$(3.27b) \qquad + \|\delta_{h,v,\mathcal{L}_h}^{n+1}\|_\Omega \,.$$

Here,

$$(3.27c) \qquad \partial_\tau \widehat{u}^{n+1} = \tfrac{1}{\tau}(\widehat{u}^{n+1} - \widehat{u}^n)$$

denotes the discrete time derivative of a function $\widehat{u}$.

Proof. Solving the error recursion (3.26) with the discrete variation-of-constants formula yields

$$e_h^{n+1} = \mathcal{R}^{n+1} e_h^0 + \tau \sum_{j=0}^{n} \mathcal{R}^{n-j} \mathcal{R}_-^{-1} \delta_h^{j+1}$$

(3.28)

$$= \mathcal{R}^{n+1} e_h^0 + \tau \sum_{j=0}^{n} \mathcal{R}^{n-j} \mathcal{R}_-^{-1} \delta_{h,s}^{j+1} + \sum_{j=0}^{n} \mathcal{R}^{n-j} (\mathcal{R} - \mathcal{I}) \delta_{h,\mathcal{L}_h}^{j+1},$$

since

$$\tau \mathcal{R}_-^{-1} \mathcal{L}_h \delta_{h,\mathcal{L}_h}^{j+1} = \mathcal{R}_-^{-1} (\mathcal{R}_+ - \mathcal{R}_-) \delta_{h,\mathcal{L}_h}^{j+1} = (\mathcal{R} - \mathcal{I}) \delta_{h,\mathcal{L}_h}^{j+1}.$$

Now we use the well-known summation by parts formula: for suitable sequences $\{\rho_j\}_j$ and $\{\delta_j\}_j$ we have

(3.29) $$\sum_{j=0}^{n} \rho_{n-j} \delta_{j+1} = r_n \delta_1 + \sum_{j=1}^{n} r_{n-j}(\delta_{j+1} - \delta_j), \qquad r_k = \sum_{j=0}^{k} \rho_j.$$

For $\rho_k = \mathcal{R}^k(\mathcal{R} - \mathcal{I})$, this yields $r_k = \mathcal{R}^{k+1} - \mathcal{I}$ and

$$\sum_{j=0}^{n} \mathcal{R}^{n-j} (\mathcal{R} - \mathcal{I}) \delta_{h,\mathcal{L}_h}^{j+1} = \mathcal{R}^{n+1} \delta_{h,\mathcal{L}_h}^1 - \delta_{h,\mathcal{L}_h}^{n+1} + \tau \sum_{j=1}^{n} \mathcal{R}^{n-j+1} \partial_\tau \delta_{h,\mathcal{L}_h}^{j+1}.$$

The bounds (3.19a) and (3.19b) imply (3.27b), since the first component of the defect $\delta_{h,\mathcal{L}_h}$ vanishes.   □

For the discrete time-derivative (3.27c) of a sufficiently smooth function u, a simple calculation shows the representations

(3.30) $$\partial_\tau \widehat{u}^{n+1} = \int_0^1 \partial_t u(t^n + \tau s) \, ds, \qquad \partial_\tau^2 \widehat{u}^{n+1} = \int_{-1}^1 (1 - |s|) \partial_t^2 u(t^n + \tau s) \, ds.$$

Note that the avarage $\partial_t \widehat{u}^{n+1/2}$ corresponds to the trapezoidal rule applied to the first integral in (3.30). It is well-known that the error

(3.31a) $$\delta_{\mathrm{tr},u}^{n+1} = \partial_\tau \widehat{u}^{n+1} - \partial_t \widehat{u}^{n+1/2}$$

satisfies

(3.31b) $$\|\delta_{\mathrm{tr},u}^{n+1}\|_\Omega \le \frac{\tau^2}{8} \int_0^1 \|\partial_t^3 u(t^n + \tau s)\|_\Omega \, ds .$$

Moreover, we define

(3.32a) $$\boldsymbol{\varphi} = \varphi(-\tau^2 \mathcal{L}_{v,h} \chi_m \mathcal{L}_{u,h}), \qquad \text{with} \qquad \varphi(z) = \frac{\Theta(z) - 1}{z}, \qquad z > 0,$$

and set $\varphi(0) = \Theta'(0)$. In addition, we will use

(3.32b) $$\widetilde{\boldsymbol{\varphi}} = \varphi(-\tau^2 \chi_m \mathcal{L}_{u,h} \mathcal{L}_{v,h} \chi_m).$$

Note that the nonzero eigenvalues of $\chi_m \mathcal{L}_{u,h} \mathcal{L}_{v,h} \chi_m$ and $\mathcal{L}_{v,h} \chi_m \mathcal{L}_{u,h}$ coincide.

Furthermore, we recall the consistency and approximation properties of the dG discretized Friedrichs' operators $\mathcal{L}_{w,h}$, with $w \in \{u, v\}$,

(3.33a) $\qquad \mathcal{L}_{w,h} w = \pi_h \mathcal{L}_w w \qquad\qquad$ for all $w \in \mathcal{D}(\mathcal{L}_w) \cap H^1(\mathcal{T}_h)^{m_w}$,

(3.33b) $\qquad \|\mathcal{L}_{w,h} e_{\pi,w}\|_\Omega \le C_{\pi,\mathcal{L},w} |h^k w|_{k+1,\mathcal{T}_h} \quad$ for all $w \in \mathcal{D}(\mathcal{L}_w) \cap H^{k+1}(\mathcal{T}_h)^{m_w}$,

cf. [10, 14].

To derive a representation of the defect δ_h^j defined in (3.25), we write (3.11) as a perturbation of the Crank-Nicolson scheme.

LEMMA 3.11. *The operators $\mathcal{R}_\pm$ defined in (3.11) satisfy*

(3.34a) $\qquad\qquad\qquad \mathcal{R}_\pm = \mathcal{R}_{\pm,\mathrm{CN}} + \mathcal{L}_h \mathcal{D}_{\mathrm{LTI}},$

where we have

(3.34b) $\qquad \mathcal{R}_{\pm,\mathrm{CN}} = \mathcal{I} \pm \frac{\tau}{2} \mathcal{L}_h \quad and \quad \mathcal{D}_{\mathrm{LTI}} = \tau^2 \begin{pmatrix} 0 & 0 \\ 0 & \frac{1}{4}\chi_{\mathrm{lf}} \mathcal{I}_v - \widetilde{\varphi}\chi_m \end{pmatrix} \mathcal{L}_h.$

Proof. The resprentation follows from the definiton of φ in (3.32a) and $\chi_m = \chi_m^2$ since

$$\Theta = \mathcal{I}_u - \tau^2 \mathcal{L}_{v,h} \chi_m \mathcal{L}_{u,h} \varphi = \mathcal{I}_u - \tau^2 \mathcal{L}_{v,h} \chi_m \widetilde{\varphi} \chi_m \mathcal{L}_{u,h},$$

where the second equality follows from [21, Cor. 1.34]. $\qquad\qquad\qquad\qquad$ □

With Lemma 3.11, we can split the defect δ_h^j defined in (3.25) as

(3.35a) $\qquad\qquad\qquad\qquad \delta_h^j = \delta_{h,\mathrm{CN}}^j + \mathcal{L}_h \delta_{h,\mathrm{LTI}}^j$

with

(3.35b) $\qquad\qquad \delta_{h,\mathrm{CN}}^j = \pi_h \partial_\tau \widehat{x}^j - \mathcal{L}_h \pi_h \widehat{x}^{j-1/2} - g_h^{j-1/2},$

$\qquad\qquad\qquad \delta_{h,\mathrm{LTI}}^j = \mathcal{D}_{\mathrm{LTI}} \pi_h \partial_\tau \widehat{x}^j$

(3.35c) $\qquad\qquad\qquad\quad = \mathcal{D}_{\mathrm{LTI}} \partial_\tau \widehat{x}^j - \mathcal{D}_{\mathrm{LTI}} \partial_\tau e_\pi^j.$

The first component of $\delta_{h,\mathrm{LTI}}^j$ vanishes such that we can apply Theorem 3.10 later.

We now have to bound the defect (3.35a). Following [14, Lemma 12.2] the defect (3.35b) stemming from the Crank-Nicolson scheme can be bounded under appropriate regularity assumptions on the exact solution of (2.1) as

(3.36) $\qquad \|\delta_{h,\mathrm{CN}}^j\|_\Omega \le C_{\pi,\mathcal{L}} |h^k \widehat{w}^{j-1/2}|_{k+1,\mathcal{T}_h} + \frac{\tau^2}{8} \int_0^1 \|\partial_t^3 v(t^{j-1} + \tau s)\|_\Omega \, ds.$

To bound the defect (3.35c) we need a bound on φ introduced in (3.32a).

DEFINITION 3.12. *With β_Ψ from Definition 3.3, we define C_φ as the smallest constant such that for φ defined in (3.32a) it holds*

(3.37) $\qquad\qquad\qquad |\varphi(z)| \le C_\varphi \qquad for\ all\ z \in [0, \beta_\Psi^2] \cap \mathbb{R}.$

Note that such a bound exists since φ is continuous on $[0, \beta_\Psi^2]$ and hence bounded.

Now we are able to state a bound for the defect (3.35c) under appropriate regularity assumptions on the exact solution of (2.1).

LEMMA 3.13. *Let* $x = \begin{pmatrix} u & v \end{pmatrix}$ *with*

$$x \in C(t^0, T; D(\mathcal{L}) \cap H^{k+1}(\mathcal{T}_h)^m) \cap C^3(t^0, T; L^2(\Omega)^m)$$

be the solution of (2.1) *and* $\tau \le \tau_{\mathrm{CFL}, \Psi}$ *defined in* (3.4). *We further assume*

$$g_v \in C^2(t^0, T; L^2(\Omega)^{m_v}).$$

Then the defect (3.35c) *is bounded by*

(3.38a) $\qquad \|\delta_{h,\mathrm{LTI}}^{n+1}\|_\Omega \le \tau^2 \widehat{C}_\varphi \Big(C_{\pi,\mathcal{L}} |h^k \partial_\tau \widehat{u}^{n+1}|_{k+1,\mathcal{T}_h} + \int_0^1 \|\partial_t^2 v(t^n + \tau s)\|_\Omega \, \mathrm{d}s$

$$+ \int_0^1 \|\partial_t g_v(t^n + \tau s)\|_\Omega \, \mathrm{d}s \Big)$$

(3.38b) $\qquad \|\partial_\tau \delta_{h,\mathrm{LTI}}^{n+1}\|_\Omega \le \tau^2 \widehat{C}_\varphi \Big(C_{\pi,\mathcal{L}} |h^k \partial_\tau^2 \widehat{u}^{n+1}|_{k+1,\mathcal{T}_h} + \int_{-1}^1 \|\partial_t^3 v(t^n + \tau s)\|_\Omega \, \mathrm{d}s$

$$+ \int_{-1}^1 \|\partial_t^2 g_v(t^n + \tau s)\|_\Omega \, \mathrm{d}s \Big)$$

with $\widehat{C}_\varphi = \sqrt{2} \max\{\frac{1}{4}, C_\varphi\}$.

Proof. With (3.33a), (3.33b), (3.37), and (2.1) we get

$$\begin{aligned}
\|\delta_{h,\mathrm{LTI}}^{n+1}\|_\Omega \le{} & \tfrac{\tau^2}{4} \|\chi_{\mathrm{lf}} \pi_h \partial_\tau \partial_t \widehat{v}^{n+1}\|_\Omega + \tau^2 C_\varphi \|\chi_m \pi_h \partial_\tau \partial_t \widehat{v}^{n+1}\|_\Omega \\
& + \tfrac{\tau^2}{4} \|\chi_{\mathrm{lf}} \pi_h \partial_\tau g_v^{n+1}\|_\Omega + \tau^2 C_\varphi \|\chi_m \pi_h \partial_\tau g_v^{n+1}\|_\Omega \\
& + \tau^2 C_\varphi C_{\pi,\mathcal{L}} |\chi_m h^k \partial_\tau \widehat{u}^{n+1}|_{k+1,\mathcal{T}_h} + \tfrac{\tau^2}{4} C_{\pi,\mathcal{L}} |\chi_{\mathrm{lf}} h^k \partial_\tau \widehat{u}^{n+1}|_{k+1,\mathcal{T}_h}
\end{aligned}$$

and in the same manner

$$\begin{aligned}
\|\partial_\tau \delta_{h,\mathrm{LTI}}^{n+1}\|_\Omega \le{} & \tfrac{\tau^2}{4} \|\chi_{\mathrm{lf}} \pi_h \partial_\tau^2 \partial_t \widehat{v}^{n+1}\|_\Omega + \tau^2 C_\varphi \|\chi_m \pi_h \partial_\tau^2 \partial_t \widehat{v}^{n+1}\|_\Omega \\
& + \tfrac{\tau^2}{4} \|\chi_{\mathrm{lf}} \pi_h \partial_\tau^2 g_v^{n+1}\|_\Omega + \tau^2 C_\varphi \|\chi_m \pi_h \partial_\tau^2 g_v^{n+1}\|_\Omega \\
& + \tau^2 C_\varphi C_{\pi,\mathcal{L}} |\chi_m h^k \partial_\tau^2 \widehat{u}^{n+1}|_{k+1,\mathcal{T}_h} + \tfrac{\tau^2}{4} C_{\pi,\mathcal{L}} |\chi_{\mathrm{lf}} h^k \partial_\tau^2 \widehat{u}^{n+1}|_{k+1,\mathcal{T}_h} \ .
\end{aligned}$$

Using (3.30) completes the proof. $\qquad\square$

Now we state our main theorem which yields under certain regularity assumptions convergence of order two in time and order k in space if we choose as dG polynomial degree k.

THEOREM 3.14. *By the same regularity assumptions as in Lemma* 3.13 *together with* $\tau \le \min\{\tau_{\mathrm{CFL,lf,c}}, \tau_{\mathrm{CFL},\Psi}\}$ *and* $x_h^0 = \pi_h x(t^0)$, *the error of the full discretization satisfies*

(3.39) $\qquad\qquad \|x(t^{n+1}) - x_h^{n+1}\|_\Omega \le C(\tau^2 + h_{\max}^k)$

with a constant C *independent of* τ *and* h.

Proof. The projection error in (3.24) is bounded by

$$\|e_\pi^{n+1}\|_\Omega \le C_\pi |h^{k+1} \widehat{x}^{n+1}|_{k+1,\mathcal{T}_h},$$

cf. [14, Lemma 3.2]. With Theorem 3.10, Lemma 3.13, and $x_h^0 = \pi_h \widehat{x}^0$ we get for the discretization error

$$\|e_h^{n+1}\|_\Omega \leq C_{stb,\,c}\left(\tau \sum_{j=1}^{n+1} \|\delta_{h,s}^j\|_\Omega + \|\delta_{h,v,\mathcal{L}_h}^1\|_\Omega + \tau \sum_{j=2}^{n+1} \|\partial_\tau \delta_{h,v,\mathcal{L}_h}^j\|_\Omega\right) + \|\delta_{h,v,\mathcal{L}_h}^{n+1}\|_\Omega$$

$$\leq C_{stb,\,c}\bigg(\frac{\tau^2}{8}\|\partial_t^3 x\|_{L^1([t^0,T],L^2(\Omega))}$$

$$+ 2\tau^2 \widehat{C}_\varphi\Big(\|\partial_t^3 v\|_{L^1([t^0,T],L^2(\Omega))} + \|\partial_t^2 g_v\|_{L^1([t^0,T],L^2(\Omega))}\Big)$$

$$+ \widehat{C}_\varphi C_{\pi,\mathcal{L}} \max_{j=0,\dots,n} |h^k \tau^2 \partial_\tau \widehat{u}^{j+1}|_{k+1,\mathcal{T}_h}$$

$$+ \widehat{C}_\varphi \tau^2 \Big(\max_{s\in[t^0,T]} \|\partial_t^2 v(s)\|_\Omega + \max_{s\in[t^0,T]} \|\partial_t^1 g_v(s)\|_\Omega\Big)$$

$$+ C_{\pi,\mathcal{L}} \tau \sum_{j=0}^{n} |h^k \widehat{x}^{j+1/2}|_{k+1,\mathcal{T}_h} + \widehat{C}_\varphi C_{\pi,\mathcal{L}} \tau \sum_{j=1}^{n} |h^k \tau^2 \partial_\tau^2 \widehat{u}^{j+1}|_{k+1,\mathcal{T}_h}\bigg).$$

This proves the statement.   □

Remark 3.15. If we use the midpoint evaluation $g_h^{n+1/2} = g_h(t^{n+1/2})$ in (3.6) instead of the average (3.7), we get an additional term $\tau^2 \|\partial_t^2 g\|_{L^1([t^0,T],L^2(\Omega))}$ in the bound of Theorem 3.14. Nevertheless, this modification leads to the same order of convergence.

3.3. Stability and convergence of local time-integration schemes. So far, we proved our theoretical results for general filter functions Ψ. In this section, we investigate the constants from Definition 3.3 for the special case of using leapfrog-Chebychev polynomials and for a rational function from our previous work [5, 6].

We start with considering the locally-implicit method from [24], where, for all $z \in [0, \infty)$, it holds

$$(3.40) \qquad \Psi(z) = (1 + \tfrac{z}{4})^{-1} > 0, \qquad \Theta(z) = 1, \qquad \varphi(z) = 0.$$

Thus we obtain $\beta_\Psi = \infty$ with the constants $c_\Theta = 1$ and $C_\varphi = 0$. Inserting these constants into Definition 3.4 we get exactly the CFL conditions from the literature, i.e., [14, Assumption 11.26] for Friedrichs' systems or from [24] for the special case of Maxwells equations. This indicates, that our new general theory does not require stronger assumptions than for the known results.

Now we turn to the new local time-stepping methods. Here, motivated by [5], we choose the filter function as the following polynomial of degree p

$$(3.41) \qquad \Psi(z)z = P_p(z)z = 2 - \frac{2}{T_p(\nu_p)}T_p\Big(\nu_p - \frac{z}{\alpha_p}\Big), \qquad \alpha_p = 2\frac{T_p'(\nu_p)}{T_p(\nu_p)},$$

with a stabilization parameter $\nu_p > 1$. With T_p, we denote the pth Chebychev polynomial of first kind.

THEOREM 3.16. *Let Ψ be given by (3.41) for some $p \in \mathbb{N}$ and $\nu_p > 1$. If we choose*

$$(3.42a) \qquad c_\Theta = \tfrac{1}{2}\big(1 - \tfrac{1}{T_p(\nu_p)}\big) \in (0, \tfrac{1}{2}),$$

then, (3.12) *and* (3.37) *are satisfied for*

$$(3.42b) \qquad \beta_\Psi^2 = \alpha_p(\nu_p + 1) \qquad and \qquad C_\varphi = \tfrac{1}{4}\Big(\tfrac{1}{c_\Theta} - 1\Big).$$

Proof. Following [5, Lemmas 5.1, 5.4] we have

$$\Psi(z)z \le 4(1 - c_\Theta), \qquad 0 < \Psi(z) \le 1, \qquad 0 \le z \le \beta_\Psi^2$$

and hence

$$\Theta(z) = \Psi(z)^{-1}\big(1 - \tfrac{z}{4}\Psi(z)\big) \ge 1 - \tfrac{z}{4}\Psi(z) \ge c_\Theta \ .$$

The formula for C_φ can be shown analogously to the proof of [5, Lemma 5.4]. □

Note that for $p = 1$ we have $\Psi \equiv 1$ and the scheme (3.6) is just the leapfrog method (which is independent of the stabilization parameter ν_p). If we choose $c_\Theta = 1 - \vartheta^2$, for $\vartheta^2 \in (0,1)$, we get $\beta_\Psi^2 = 4(1 - c_\Theta) = 4\vartheta^2$.

We collect all relevant details on the different LTI schemes and their constants in Table 1.

If, for $p \ge 2$, we choose

$$(3.43) \qquad \qquad \nu_p = 1 + \frac{\eta^2}{2p^2}, \qquad \eta > 0,$$

then c_Θ defined in (3.42a) can be bounded independently of p, see [5, Lemma 5.5] for a more in-depth view. In this case it holds

$$\beta_\Psi^2 = \beta_p^2 \ge 2p \ge 4.$$

Thus, the assumption of Lemma 3.7 on Ψ is satisfied for the leapfrog-Chebychev polynomials (3.41).

Remark 3.17 (Implementation).
(a) It is important to note that one does not have to evaluate the polynomials (3.41) of degree $p - 1$ in each step. Instead one calculates the action of a vector $\mathbf{u}$ on $\Psi(-\tau^2 \mathbf{A}_m)$ in an efficient way by a three-term recurrence relation, see [3, Algo. 4.2] for details. Here $\mathbf{A}_m$ denotes the system matrix of $\mathcal{L}_{v,h}\chi_m\mathcal{L}_{u,h}$ one obtains after choosing an appropriate basis of the dG space $\mathbb{V}_h$, see [25].
(b) By sorting the degrees-of-freedom in an appropriate way [25, 31] one can see that $\Psi(-\tau^2 \mathbf{A}_m)$ only acts on the few fine elements in $\mathcal{T}_{h,f}$ plus two additional layers.

4. Numerical examples. At last, we verify our findings numerically with three examples. First we substantiate the error bounds of Theorem 3.14 and we study the influence of stabilization of the leapfrog-Chebychev local time-stepping (LFC-LTS) method. Afterwards, we investigate the efficiency of the LFC-LTS method compared to the locally implicit (LI) and the original leapfrog scheme. The linear systems in the LI method are solved with the conjugate gradient method without preconditioning since it required only a few iterations (not more than four in our examples). Note that it is essential to run the conjugate gradient method with the correct inner-product induced by the mass matrix.

The codes to reproduce our results are available at

https://gitlab.kit.edu/malik.scheifinger/dg-lts-maxwell

The software is based on the FEM library `deal.II` [2] at version 9.5 and the Maxwell toolbox `TiMaxdG` [4]. Since we use `deal.II`, all our examples are done with rectangular mesh elements.

4.1. Linear Maxwells equations. Linear Maxwells equations in transverse-electric (TE) mode, see [28, §2.3], are given by

$$
\begin{align}
(4.1a) && \varepsilon\partial_t E_x &= \partial_y H_z - J_x, && \Omega \times (0,T), \\
(4.1b) && \varepsilon\partial_t E_y &= -\partial_x H_z - J_y, && \Omega \times (0,T), \\
(4.1c) && \mu\partial_t H_z &= \partial_y E_x - \partial_x E_y, && \Omega \times (0,T), \\
(4.1d) && E(0) &= E^0, \quad H(0) = H^0, && \Omega, \\
(4.1e) && E \times \mathbf{n} &= 0, && \partial\Omega \times (0,T).
\end{align}
$$

As computational spatial domain we choose $\Omega = (0,1)^2$ and final time $T = 1$. We set $\varepsilon = \mu = 1$ and use initial values

$$
\begin{align}
(4.2a) && E_x^0(x,y,t) &= \cos(2\pi x)\sin(2\pi y), \\
(4.2b) && E_y^0(x,y,t) &= -\sin(2\pi x)\cos(2\pi y), \\
(4.2c) && H_z^0(x,y,t) &= 4\pi\cos(2\pi x)\cos(2\pi y),
\end{align}
$$

as well as right-hand sides

$$
\begin{align}
(4.3a) && J_x(x,y,t) &= -(1 + 8\pi^2)\cos(2\pi x)\sin(2\pi y)\mathrm{e}^t, \\
(4.3b) && J_y(x,y,t) &= (1 + 8\pi^2)\sin(2\pi x)\cos(2\pi y)\mathrm{e}^t.
\end{align}
$$

The exact solution to (4.1) with (4.2) and (4.3) is given by a variant of the cavity solution [24]

$$
\begin{align}
(4.4a) && E_x(x,y,t) &= \cos(2\pi x)\sin(2\pi y)\mathrm{e}^t, \\
(4.4b) && E_y(x,y,t) &= -\sin(2\pi x)\cos(2\pi y)\mathrm{e}^t, \\
(4.4c) && H_z(x,y,t) &= 4\pi\cos(2\pi x)\cos(2\pi y)\mathrm{e}^t.
\end{align}
$$

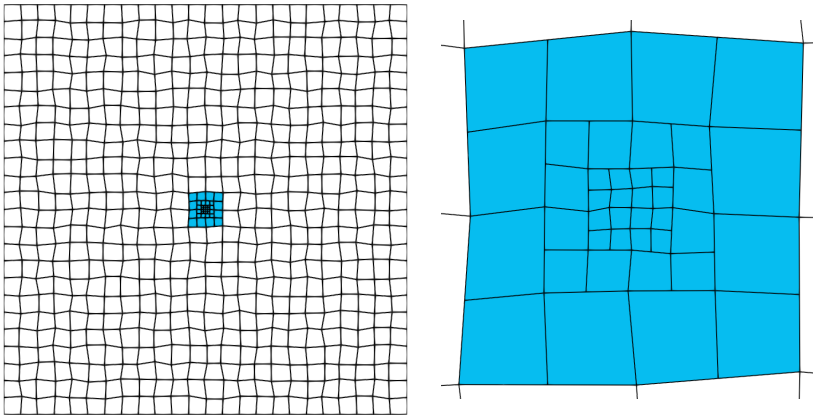Thereby we can compute the exact L^2-error of our scheme.

Figure 1: Locally refined mesh of the domain $(0,1)^2$.

We use the spatial mesh illustrated in Figure 1 in which we apply threefold refinement in the blue central box. The mesh has been randomly perturbed to counteract super convergence effects of the space discretization. Moreover, the dG degree is choosen as $k = 5$.
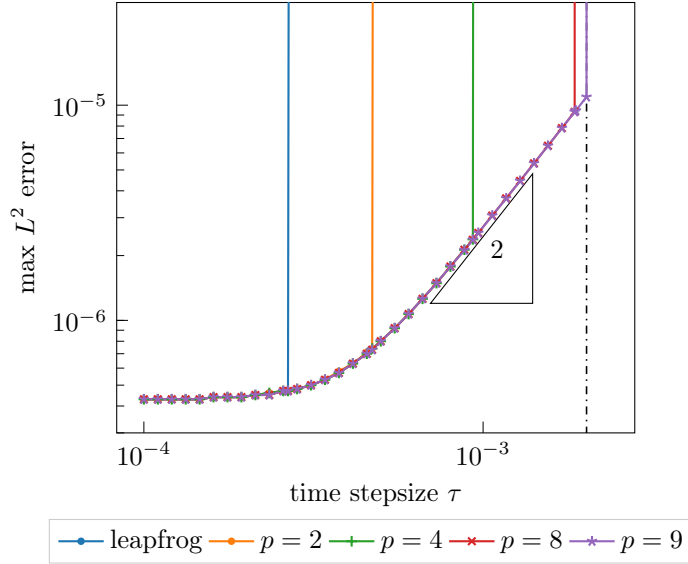
Figure 2: Error of the numerical solution of (4.1) with initial data given by (4.4) obtained by the leapfrog method (blue) and the local time-stepping method (3.6) with filter (3.41), polynomial degrees $p = 2$ (orange), $p = 4$ (green), $p = 8$ (red), $p = 9$ (purple), and stabilization (3.43) with $\eta = 1$. The space discretization is done with dG degree $k = 5$ and a three times at the center locally refined mesh, see Figure 1. The dash-dotted line depicts the maximal stable time stepsize of leapfrog method used on the coarse mesh $\mathcal{T}_{h,\mathrm{lf}}$.

4.2. Order of convergence. We apply the LTS method (3.6) with the LFC filter (3.41) and the stabilization parameter (3.43) for $\eta = 1$ and various values of p.

In Figure 2, we illustrate the stability and convergence behavior with LFC polynomials of degrees $p = 2, 4, 8, 9$. We observe second-order convergence in time until the error reaches a plateau stemming from the spatial discretization. Moreover, we see that an increase of p weakens the CFL condition significantly compared to the leapfrog method (blue). Obviously one can not exceed the maximal stable time stepsize of the leapfrog method on the coarse part $\mathcal{T}_{h,\mathrm{lf}}$.

4.3. Necessity of stabilization. In this example we show that stabilization, i.e., choosing $\eta > 0$, is indispensable in the LFC-LTS method, see also [5] for second-order differential equations. For this we consider the following one-dimensional example

$$
\begin{align}
(4.5\mathrm{a}) \qquad & \partial_t u = -\partial_x v, & \Omega \times (0,T), \\
(4.5\mathrm{b}) \qquad & \partial_t v = -\partial_x u, & \Omega \times (0,T), \\
(4.5\mathrm{c}) \qquad & u(0) = u^0, \quad v(0) = v^0, & \Omega, \\
(4.5\mathrm{d}) \qquad & u = 0, & \partial\Omega \times (0,T),
\end{align}
$$

on $\Omega = (0,1)$. We choose the initial values such that

$$
\begin{align}
u(x,t) &= \sin(2\pi x)\cos(2\pi t) \\
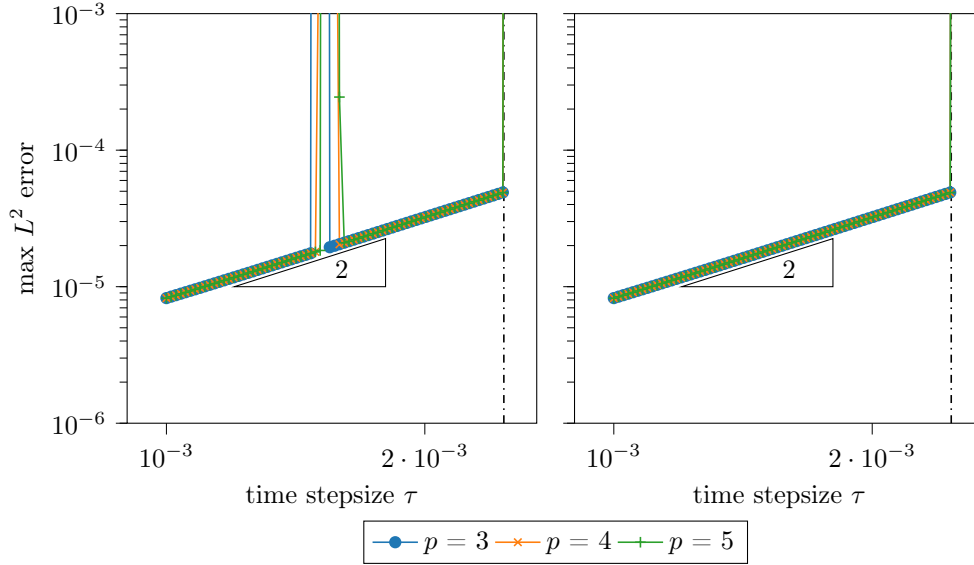v(x,t) &= -\cos(2\pi x)\sin(2\pi t).
\end{align}
$$

Figure 3: Error of the LFC-LTS method for the example in Section 4.3 with polynomial degrees $p = 3, 4, 5$. Left: without stabilization ($\eta = 0$), right: with stabilization ($\eta = 0.1$). The dash-dotted line depicts the maximal stable time-stepsize of the leapfrog method on the coarse mesh $\mathcal{T}_{h,\mathrm{lf}}$.

is the exact solution of (4.5).

We use a spatial grid where all cells have diameter $h_{\max} = 0.009975$ except for one cell in the middle of Ω with diameter $h_{\min} = 0.0025 \approx h_{\max}/4$. In Figure 3 we show the error of the LFC-LTS method with polynomial degrees $p = 3, 4, 5$ and stabilization (3.43) with $\eta = 0$ and $\eta = 0.1$, on the left and the right picture, respectively. As we can see, for $\eta = 0$, the method becomes unstable for certain time stepsizes whereas the slightly stabilized method with $\eta = 0.1$ has no deviations.

4.4. Runtime comparison. Next, we compare the runtimes of the LFC-LTS method, the LI method, and the leapfrog method at two different examples. We revisit (4.1) on $\Omega = (0, 4)^2$ and use an equidistant spatial grid with $h \approx 0.022$. For the dG space we use the polynomial degree $k = 2$. Cells with center in the ball $\|x\| \leq r$ with $r \in \{0.1, 0.5\}$ are refined twice. The minimal mesh diameter on the whole mesh is $h_{\min} \approx 0.0055$. Moreover we select the time-stepsize $\tau = 0.0022$ which is small enough to balance time and space discretization errors. For $r = 0.1$ and $r = 0.5$ the L^2 errors are $4 \cdot 10^{-4}$ and $7.6 \cdot 10^{-4}$, respectively for all three methods.

In Table 2, we summarize the runtimes of the leapfrog, LI, and LFC-LTS method for the two values of r. For the leapfrog method we choose the maximum stable stepsize $\tau = 6.8 \cdot 10^{-4}$. For the LFC-LTS scheme, we choose the LFC polynomial degree $p = 4$ and $\tau = 2.2 \cdot 10^{-3}$.

For $r = 0.1$, the two local time-integration schemes LI and LFC-LTS clearly outperform the leapfrog method, with the LFC-LTS method being more than twice as fast. In the second example, where $r = 0.5$, the percentage of dofs in the refined region is still relatively large, so that the computational cost for solving the linear

	$r = 0.1$		$r = 0.5$	
total dofs	1 782 756		2 097 522	
refined dofs	15 012	0.84%	353 430	16.85%
runtime leapfrog	71.1sec	100.0%	85.1sec	100.0%
runtime LI	53.7sec	75.5%	93.0sec	109.3%
runtime LFC-LTS	34.1sec	48.0%	57.5sec	67.6%

Table 2: Runtime comparison between the leapfrog, LI and LFC-LTS methods on two different examples explained in Section 4.4.

system in the LI method is significant. Here, the leapfrog method is slighly faster than the LI method but much slower than the LFC-LTS method.

Overall we see that the LFC-LTS method performs better than the leapfrog and the LI method in both scenarios.

REFERENCES

[1] M. ALMQUIST AND M. MEHLIN, *Multilevel local time-stepping methods of Runge-Kutta-type for wave equations*, SIAM J. Sci. Comput., 39 (2017), pp. A2020–A2048, https://doi.org/10.1137/16M1084407.

[2] D. ARNDT, W. BANGERTH, M. BERGBAUER, M. FEDER, M. FEHLING, J. HEINZ, T. HEISTER, L. HELTAI, M. KRONBICHLER, M. MAIER, P. MUNCH, J.-P. PELTERET, B. TURCKSIN, D. WELLS, AND S. ZAMPINI, *The deal.II library, version 9.5*, Journal of Numerical Mathematics, 31 (2023), pp. 231–246, https://doi.org/10.1515/jnma-2023-0089.

[3] C. CARLE, *On leapfrog-Chebyshev schemes for second-order differential equations*, PhD thesis, Karlsruhe Institute of Technology (KIT), 2021, https://doi.org/10.5445/IR/1000147725.

[4] C. CARLE, J. DÖRNER, J. KÖHLER, AND B. MAIER, *TiMaxdG*, https://gitlab.kit.edu/kit/ianm/ag-numerik/projects/dg-maxwell/timaxdg.

[5] C. CARLE AND M. HOCHBRUCK, *Error analysis of multirate leapfrog-type methods for second-order semilinear ODEs*, SIAM J. Numer. Anal., 60 (2022), pp. 2897–2924, https://doi.org/10.1137/21M1427255.

[6] C. CARLE AND M. HOCHBRUCK, *Error analysis of second-order local time integration methods for discontinuous Galerkin discretizations of linear wave equations*, Math. Comp., (2024), pp. 1–31, https://doi.org/10.1090/mcom/3952.

[7] S. DESCOMBES, S. LANTERI, AND L. MOYA, *Locally implicit time integration strategies in a discontinuous Galerkin method for Maxwell's equations*, J. Sci. Comput., 56 (2013), pp. 190–218, https://doi.org/10.1007/s10915-012-9669-5.

[8] S. DESCOMBES, S. LANTERI, AND L. MOYA, *High-order locally implicit time integration strategies in a discontinuous Galerkin method for Maxwell's equations*, in Spectral and high order methods for partial differential equations—ICOSAHOM 2012, vol. 95 of Lect. Notes Comput. Sci. Eng., Springer, Cham, 2014, pp. 205–215, https://doi.org/10.1007/978-3-319-01601-6_16.

[9] S. DESCOMBES, S. LANTERI, AND L. MOYA, *Temporal convergence analysis of a locally implicit discontinuous Galerkin time domain method for electromagnetic wave propagation in dispersive media*, J. Comput. Appl. Math., 316 (2017), pp. 122–132, https://doi.org/10.1016/j.cam.2016.09.038.

[10] D. A. DI PIETRO AND A. ERN, *Mathematical aspects of discontinuous Galerkin methods*, vol. 69 of Mathématiques & Applications (Berlin) [Mathematics & Applications], Springer, Heidelberg, 2012, https://doi.org/10.1007/978-3-642-22980-0.

[11] J. DIAZ AND M. J. GROTE, *Energy conserving explicit local time stepping for second-order wave equations*, SIAM J. Sci. Comput., 31 (2009), pp. 1985–2014, https://doi.org/10.1137/070709414.

[12] J. Diaz and M. J. Grote, *Multi-level explicit local time-stepping methods for second-order wave equations*, Comput. Methods Appl. Mech. Engrg., 291 (2015), pp. 240–265, https://doi.org/10.1016/j.cma.2015.03.027.

[13] V. Dolean, H. Fahs, L. Fezoui, and S. Lanteri, *Locally implicit discontinuous Galerkin method for time domain electromagnetics*, J. Comput. Phys., 229 (2010), pp. 512–526, https://doi.org/10.1016/j.jcp.2009.09.038.

[14] W. Dörfler, M. Hochbruck, J. Köhler, A. Rieder, R. Schnaubelt, and C. Wieners, *Wave Phenomena: Mathematical Analysis and Numerical Approximation*, vol. 49 of Oberwolfach Seminars, Springer International Publishing, Cham, 2023, https://link.springer.com/10.1007/978-3-031-05793-9.

[15] A. Ern and J.-L. Guermond, *Finite elements III—first-order and time-dependent PDEs*, vol. 74 of Texts in Applied Mathematics, Springer, Cham, [2021] ©2021, https://doi.org/10.1007/978-3-030-57348-5.

[16] M. J. Grote, M. Mehlin, and T. Mitkova, *Runge-Kutta-based explicit local time-stepping methods for wave propagation*, SIAM J. Sci. Comput., 37 (2015), pp. A747–A775, https://doi.org/10.1137/140958293.

[17] M. J. Grote, S. Michel, and S. A. Sauter, *Stabilized leapfrog based local time-stepping method for the wave equation*, Math. Comp., 90 (2021), pp. 2603–2643, https://doi.org/10.1090/mcom/3650.

[18] M. J. Grote and T. Mitkova, *Explicit local time-stepping methods for Maxwell's equations*, J. Comput. Appl. Math., 234 (2010), pp. 3283–3302, https://doi.org/10.1016/j.cam.2010.04.028.

[19] M. J. Grote and T. Mitkova, *Explicit local time-stepping methods for time-dependent wave propagation*, in Direct and inverse problems in wave propagation and applications, vol. 14 of Radon Ser. Comput. Appl. Math., De Gruyter, Berlin, 2013, pp. 187–218, https://doi.org/10.1515/9783110282283.187.

[20] M. J. Grote and T. Mitkova, *High-order explicit local time-stepping methods for damped wave equations*, J. Comput. Appl. Math., 239 (2013), pp. 270–289, https://doi.org/10.1016/j.cam.2012.09.046.

[21] N. J. Higham, *Functions of matrices*, Society for Industrial and Applied Mathematics (SIAM), Philadelphia, PA, 2008, https://doi.org/10.1137/1.9780898717778. Theory and computation.

[22] M. Hochbruck and J. Köhler, *Error analysis of discontinuous Galerkin discretizations of a class of linear wave-type problems*, in Mathematics of Wave Phenomena, W. Dörfler, M. Hochbruck, D. Hundertmark, W. Reichel, A. Rieder, R. Schnaubelt, and B. Schörkhuber, eds., Trends in Mathematics, Birkhäuser Basel, Oct 2020, pp. 197–218, https://doi.org/10.1007/978-3-030-47174-3_12.

[23] M. Hochbruck and J. Köhler, *Error analysis of a fully discrete discontinuous Galerkin alternating direction implicit discretization of a class of linear wave-type problems*, Numer. Math., 150 (2022), pp. 893–927, https://doi.org/10.1007/s00211-021-01262-z.

[24] M. Hochbruck and A. Sturm, *Error analysis of a second-order locally implicit method for linear Maxwell's equations*, SIAM J. Numer. Anal., 54 (2016), pp. 3167–3191, https://doi.org/10.1137/15M1038037.

[25] M. Hochbruck and A. Sturm, *Upwind discontinuous Galerkin space discretization and locally implicit time integration for linear Maxwell's equations*, Math. Comp., 88 (2019), pp. 1121–1153, https://doi.org/10.1090/mcom/3365.

[26] M. Kotovshchikova, D. K. Firsov, and S. H. Lui, *A third-order multirate Runge-Kutta scheme for finite volume solution of 3D time-dependent Maxwell's equations*, Commun. Appl. Math. Comput. Sci., 15 (2020), pp. 65–87, https://doi.org/10.2140/camcos.2020.15.65.

[27] E. Montseny, S. Pernet, X. Ferriéres, and G. Cohen, *Dissipative terms and local time-stepping improvements in a spatial high order discontinuous Galerkin scheme for the time-domain Maxwell's equations*, J. Comput. Phys., 227 (2008), pp. 6795–6820, https://doi.org/10.1016/j.jcp.2008.03.032.

[28] J. Niegemann, *Higher-Order Methods for Solving Maxwell's Equations in the Time-Domain*. https://publikationen.bibliothek.kit.edu/1000011812, 2009, https://doi.org/10.5445/IR/1000011812.

[29] S. Piperno, *Symplectic local time-stepping in non-dissipative DGTD methods applied to wave propagation problems*, M2AN Math. Model. Numer. Anal., 40 (2006), pp. 815–841, https://doi.org/10.1051/m2an:2006035.

[30] T. Rylander and A. Bondeson, *Stability of explicit–implicit hybrid time-stepping schemes for Maxwell's equations*, J. Comput. Phys., 179 (2002), pp. 426–438, https://doi.org/https:

//doi.org/10.1006/jcph.2002.7063.

[31] A. STURM, *Locally Implicit Time Integration for Linear Maxwell's Equations*, PhD thesis, Karlsruher Institut für Technologie (KIT), 2017, https://doi.org/10.5445/IR/1000069341.

[32] J. G. VERWER, *Component splitting for semi-discrete Maxwell equations*, BIT, 51 (2011), pp. 427–445, https://doi.org/10.1007/s10543-010-0296-y.